APPLIED AND ENVIRONMENTAL MICROBIOLOGY, Feb. 2007, p. 947–955 Vol. 73, No. 3
0099-2240/07/$08.00+0 doi:10.1128/AEM.01251-06

Detection of UV-Induced Thymine Dimers in Individual *Cryptosporidium parvum* and *Cryptosporidium hominis* Oocysts by Immunofluorescence Microscopy▽

B. H. Al-Adhami,[1] R. A. B. Nichols,[1] J. R. Kusel,[2] J. O'Grady,[3] and H. V. Smith[1]*

Scottish Parasite Diagnostic Laboratory, Stobhill Hospital, Glasgow G21 3UW, United Kingdom[1]; Division of Infection & Immunity, Institute of Biomedical and Life Sciences, University of Glasgow, Glasgow G12 8QQ, United Kingdom[2]; and Strathclyde Institute of Pharmacy and Biomedical Sciences, University of Strathclyde, Glasgow G4 0NR, United Kingdom[3]

Received 31 May 2006/Accepted 25 September 2006

To investigate the effect of UV light on *Cryptosporidium parvum* and *Cryptosporidium hominis* oocysts in vitro, we exposed intact oocysts to 4-, 10-, 20-, and 40-mJ · cm^{-2} doses of UV irradiation. Thymine dimers were detected by immunofluorescence microscopy using a monoclonal antibody against cyclobutyl thymine dimers (anti-TDmAb). Dimer-specific fluorescence within sporozoite nuclei was confirmed by colocalization with the nuclear fluorogen 4′,6′-diamidino-2-phenylindole (DAPI). Oocyst walls were visualized using either commercial fluorescein isothiocyanate-labeled anti-*Cryptosporidium* oocyst antibodies (FITC-CmAb) or Texas Red-labeled anti-*Cryptosporidium* oocyst antibodies (TR-CmAb). The use of FITC-CmAb interfered with TD detection at doses below 40 mJ · cm^{-2}. With the combination of anti-TDmAb, TR-CmAb, and DAPI, dimer-specific fluorescence was detected in sporozoite nuclei within oocysts exposed to 10 to 40 mJ · cm^{-2} of UV light. Similar results were obtained with *C. hominis*. *C. parvum* oocysts exposed to 10 to 40 mJ · cm^{-2} of UV light failed to infect neonatal mice, confirming that results of our anti-TD immunofluorescence assay paralleled the outcomes of our neonatal mouse infectivity assay. These results suggest that our immunofluorescence assay is suitable for detecting DNA damage in *C. parvum* and *C. hominis* oocysts induced following exposure to UV light.

UV irradiation as a sterilization technology in the water and food industry is effective in killing contaminating organisms, such as viruses, bacteria, fungal spores, and parasites (8). The major DNA lesions caused by UV light are cyclobutyl pyrimidine dimers (CPD), which are responsible for UV-induced cytotoxicity and mutagenicity in living cells and microorganisms. UV-induced damage consists of chemical base modifications, whereby two adjacent pyrimidine residues (cytosine or thymine) form a dimer (thymine dimer [TD], cytosine dimer, or thymine-cytosine heterodimer) and 6-4 photoproducts. The formation of these lesions in genomic DNA inhibits normal replication and transcription of DNA and results in the inactivation of cells (12). However, UV-induced DNA lesions in living human epidermal cells (21) and in some unicellular microorganisms (16) can be repaired by one or more mechanisms. These mechanisms include the enzyme-dependent nucleotide excision repair, also named dark repair, and the light-dependent reaction known as photoreactivation. Dark repair and photoreactivation enable UV-inactivated microorganisms to recover, which can reduce the efficiency of UV inactivation (20).

Cryptosporidium parvum oocysts have the ability to carry out photoreactivation and dark repair at the genomic level (13, 16). Also, nucleotide excision repair genes in *C. parvum* and *Cryptosporidium hominis* have been identified. However, UV inactivation of *Cryptosporidium* oocysts is irreversible, despite the presence of these UV repair genes (18). Rochelle et al. (19) demonstrated the accumulation of cyclobutane TDs in the genome of *C. parvum* oocysts exposed to increasing dosages of UV light, using a chemiluminescent Western blot assay.

Current United Kingdom regulatory (2, 3) and nonregulatory (United Kingdom Standing Committee of Analysts) (1) and U.S. Environmental Protection Agency (EPA) (24, 25) methods for detecting the presence of *Cryptosporidium* sp. oocysts in water require that samples be analyzed by immunofluorescence and differential interference contrast (DIC) microscopy and that the identification and enumeration of oocysts be based on specific morphological, morphometric, and fluorescence criteria. Clearly, a chemiluminescent Western blot assay using soluble oocyst extracts is not suitable for detecting UV damage in individual oocysts in routine samples, as this assay cannot determine whether all oocysts in a sample exposed to UV irradiation have been disinfected.

Here, we report the development and in vitro validation of an immunofluorescence assay to detect the presence of TDs in the nuclei of individual sporozoites within intact, UV-irradiated *C. parvum* and *C. hominis* oocysts by using an anti-TD dimer monoclonal antibody (anti-TDmAb). The presence of TDs in individual irradiated oocysts was detected by immunofluorescence microscopy using a method compatible with current United Kingdom and U.S. EPA methods (3, 24, 25). To maximize TD localization in *C. parvum* and *C. hominis* oocysts, we developed a TD-labeling procedure based on repeated freezing and thawing of irradiated oocysts (14).

* Corresponding author. Mailing address: Scottish Parasite Diagnostic Laboratory, Stobhill Hospital, Glasgow G21 3UW, United Kingdom. Phone: 44 141-201-3028. Fax: 44 141-201-3029. E-mail: huw.smith@northglasgow.scot.nhs.uk.

▽ Published ahead of print on 29 September 2006.

TABLE 1. Effect of different treatments on the percent binding of anti-TDmAb to the nuclei of irradiated sporozoites

Sporozoite treatment	% Antibody binding (mean ± SD)[a]	Sporozoite morphology
Fixed in PFA or methanol and air dried	10.3 ± 4.0	Excellent
Microwaved for 2 min, fixed in PFA or methanol, and air dried	28.7 ± 7.5	Damaged
Heated in water bath at 70°C for 5 min, fixed in PFA or methanol, and air dried	63.3 ± 6.5	Damaged
Air dried overnight at room temp and then fixed in methanol	83.7 ± 7.9	Varies from good to damaged

[a] Percent antibody binding indicates the number of sporozoites with anti-TDmAb$^+$, DAPI$^+$ nuclei (n = 300 observations per sporozoite treatment).

MATERIALS AND METHODS

Parasites. Purified *C. parvum* oocysts (Iowa isolate) were purchased from Bunch Grass Farm (BGF, Idaho) and stored between 4 and 8°C until used. Recently excreted (<60-day-old) oocysts were used throughout the study. In addition, aged (purified, stored in reverse osmosis water at 4°C for 2 years) *C. parvum* (Iowa isolate; BGF, ID) oocysts were used to determine whether age and viability influenced the production of UV-induced TDs in sporozoite nuclei.

C. hominis oocysts were obtained from fecal samples of human origin submitted to the Scottish Parasite Diagnostic Laboratory for routine diagnosis. Oocysts were purified by water-ether concentration followed by sucrose floatation (5) and were genotyped at the *Cryptosporidium* oocyst wall protein (9) locus and at two 18S (15, 27, 28) loci.

C. parvum and *C. hominis* oocyst viability was determined using both the fluorogenic vital dye assay of Campbell et al. (6) and the maximized in vitro excystation assay of Robertson et al. (17).

Antibodies. The following antibodies were used: (i) mouse anti-TDmAb, immunoglobulin G (IgG) isotype (Kamiya Biomedical Co.), which reacts specifically with thymine dimers produced by UV irradiation in double-stranded DNA (dsDNA) or single-stranded DNA; its optimal dilution of 1:40 was used in all experiments; (ii) mouse anti-dsDNA monoclonal antibody (anti-dsDNAmAb, IgG isotype; Alpha Diagnostic, United Kingdom) optimally diluted to 1:40; (iii) rabbit-anti-*Cryptosporidium* sporozoite polyclonal antibody (anti-CspAb) prepared in our laboratories and optimally diluted to 1:80; (iv) fluorescein isothiocyanate (FITC)-labeled rabbit anti-mouse IgG (FITC anti-mouse IgG, 1:50 optimal dilution; Sigma, United Kingdom) or FITC-labeled mouse anti-rabbit IgG (FITC anti-rabbit IgG, 1:50 optimal dilution; Sigma, United Kingdom); (v) FITC-labeled anti-*Cryptosporidium* monoclonal antibody (FITC-CmAb, 1:20 optimal dilution, Waterborne, Inc.); and (vi) Texas Red-labeled anti-*Cryptosporidium* monoclonal antibodies (TR-CmAb, 1:20 optimal dilution; Waterborne, Inc.).

Oocyst irradiation. Approximately 1×10^6 *C. parvum* oocysts suspended in 5 ml of Hanks' balanced salt solution (HBSS) were placed in plastic petri dishes (36-mm diameters) and mixed constantly during exposure to UV light, using a magnetic stirrer. Oocysts were exposed to a low-pressure UV lamp with an output at 254 nm. The procedure was adapted from that described by Rochelle et al. (18). Short-wave UV irradiation from a UVGL-58 Mineralight lamp was used. The intensity of the UV light, measured using a digital UVX radiometer, was (on average) 350 $\mu W \cdot cm^{-2}$ at 254 nm. A rig was set up 10 cm below the lamp, and a position where the UV intensity was maximal (350 $\mu W \cdot cm^{-2}$) was marked. The UV dose was then determined as follows:

$$\text{UV dose} = \text{irradiance} \times \text{exposure time (seconds)}$$

$$mJ \cdot cm^{-2} = mW \cdot cm^{-2} \times \text{seconds}$$

To achieve different UV dosages ($mJ \cdot cm^{-2}$), oocysts were exposed to UV light for various periods of time at a constant distance (10 cm) from the constant-intensity UV source. Oocysts were exposed to 4-, 10-, 20-, or 40-$mJ \cdot cm^{-2}$ doses. For each experiment, control oocysts were exposed to the same conditions but without irradiation.

TD localization in the nuclei of irradiated sporozoites. Irradiated or control *C. parvum* oocysts were excysted in an excystation solution (1% bile in Hanks' minimum essential medium and 0.4% $NaHCO_3$ in deionized water) (17). Freshly excysted sporozoites were passed through a 3-μm membrane filter (cellulose acetate; Millipore, United Kingdom) to remove empty oocysts and other larger particulates. Five μl of filtrate was pipetted individually onto eight-well multispot microscopic slides (Hendley Essex Ltd., United Kingdom) and left to air dry overnight at room temperature (RT). Initially, air-dried sporozoites were fixed in 4% paraformaldehyde (PFA) or absolute methanol. Slides were washed and blocked with HBSS containing 0.2% Triton X-100 and 5% dried skim milk (blocking solution) for 1 h at RT. Slides were washed thoroughly in wash solution (1% dried skim milk in HBSS) and incubated for 30 min at 37°C and then overnight at 4°C with anti-TDmAb, anti-dsDNAmAb, or anti-CspAb. Slides were washed three times for 5 min each time, drained, and then incubated with the appropriate FITC-labeled antibody (anti-mouse IgG or anti-rabbit IgG) for 1 h at 37°C, followed by washing three times for 5 min each time in wash solution and then twice for 5 min each time in HBSS. Slides were counterstained with 4′,6′-diamidino-2-phenylindole (DAPI, 1:5,000 dilution; Sigma, United Kingdom) (23) for 5 min at RT and rinsed in HBSS before being air dried at RT and mounted with fluorescence antifadant medium (MDCI Ltd., United Kingdom). Slides were analyzed by both epifluorescence and Nomarski DIC microscopy (Olympus, United Kingdom).

Maximizing anti-TDmAb localization in the nuclei of excysted, irradiated sporozoites. To maximize the localization of anti-TDmAb into sporozoite nuclei, various membrane disruption treatments were tested. These included fixation of sporozoites in suspension in PFA (4%, 5 min) or methanol (absolute, 5 min) followed by air drying on microscope slides, microwaving sporozoites (650 W) for 2 min either in suspension or after air drying on microscope slides, heating sporozoites (70°C, 5 min) either in suspension or after air drying on microscope slides, and air drying sporozoites in suspension on microscope slides overnight at RT followed by methanol fixation (Table 1).

Maximizing anti-TDmAb localization in the nuclei of irradiated sporozoites within intact oocysts. The treatment used to maximize anti-TDmAb localization in the nuclei of excysted, irradiated sporozoites was not as effective when intact, irradiated oocysts were used. To study the effect of UV irradiation on the formation of thymine dimers in *Cryptosporidium* oocyst DNA, we developed a freezing and thawing method for maximizing the staining of irradiated oocysts by using the antibodies described above and DAPI; this method is a modification of the freeze-thaw protocol described by Nichols and Smith (14) for DNA extraction from *C. parvum* oocysts. Oocysts were irradiated at 4, 10, 20, or 40 $mJ \cdot cm^{-2}$ as described in "Oocyst irradiation" above. Immediately after irradiation, oocysts were washed three times in HBSS and divided into two groups. In the first group, a 200-μl volume of oocysts was placed in a 500-μl capped microcentrifuge tube and exposed to various numbers of cycles of freezing and thawing. Each cycle consisted of immersion in liquid nitrogen (LN_2) for 1 min and then thawing immediately in a 65°C water bath for 1 min. Fifty-microliter volumes of irradiated, freeze-thawed oocysts were pipetted individually onto four-well multispot microscopic slides (Hendley Essex Ltd., Loughton, Essex, United Kingdom) and left to air dry overnight at RT. In the second group, irradiated oocysts were pipetted onto four-well multispot microscopic slides and air dried overnight at RT prior to freezing and thawing. Each cycle consisted of immersion in LN_2 for 1 min and then thawing immediately for 1 min at 65°C in a hot-air oven. To maximize anti-TDmAb localization in the nuclei of irradiated sporozoites within intact oocysts, three different freezing and thawing regimens (5, 7, and 10 cycles) were investigated. Following the freeze-thaw cycles, air dried oocysts were fixed in absolute methanol at RT, and the methanol was left to evaporate at RT.

Oocysts were labeled with the primary antibodies (anti-TDmAb, anti-dsDNAmAb, or anti-CspAb) followed by their respective FITC-labeled secondary (anti-mouse IgG or anti-rabbit IgG) antibodies as described above (see "TD localization in the nuclei of irradiated sporozoites") for the sporozoite labeling procedure. After washing, oocysts were labeled using either FITC-CmAb or TR-CmAb for 30 min at 37°C. Slides were then washed in HBSS, counterstained with DAPI (1:5,000), mounted with antifadant medium, and examined by both epifluorescence and DIC microscopy. The disruption of oocysts and sporozoite release was determined following labeling with FITC-CmAb to visualize oocysts and DAPI to visualize nuclei.

Neonatal mouse infectivity assay. The neonatal mouse infectivity levels for UV irradiated and nonirradiated oocysts were determined by the procedures we published previously (11).

(i) Preparation and confirmation of infectious doses. Two samples of *C. parvum* oocysts, each containing $\sim 1 \times 10^6$ oocysts, were irradiated separately at 10 and 20 mJ · cm^{-2} as previously described. A further sample, containing $\sim 1 \times 10^6$ nonirradiated oocysts, was used to prepare the standard curve. The preparation of infectious doses involved hemocytometer enumeration of the stock oocyst suspension and its dilution in deionized water to produce suspensions containing the required number of oocysts (see "Gavage of mice and determination of infection" below) in a 10-μl volume. Quality assurance in the delivery of infectious doses was performed by delivering an infectious dose (in a 10-μl volume) into a well of a four-well multispot slide (Hendley Essex Ltd., United Kingdom) for every fifth infectious dose for each neonatal mouse group. Oocysts delivered onto welled slides were air dried, methanol fixed, stained with FITC-CmAb for 30 min at 37°C and DAPI, as described above, and then enumerated.

(ii) Gavage of mice and determination of infection. Seven groups of neonatal (<6-day-old) CD-1 mice (20 mice per group) were infected with different doses of UV-treated or control (untreated) *C. parvum* oocysts, as follows. Two groups of mice were infected with oocysts irradiated at 10 mJ · cm^{-2}; mice in the first group were dosed with 300 and the second group with 3,000 irradiated oocysts. Mice in a further two groups were each dosed with 300 or 3,000 oocysts, irradiated at 20 mJ · cm^{-2}. For the standard curve, three groups of mice were infected with nonirradiated oocysts at doses of 30, 150, or 300 oocysts per group. Mice were sacrificed 7 days postinfection, and the terminal ileum was excised, formalin fixed, embedded in paraffin, sectioned longitudinally, and stained with hematoxylin and eosin. Slides were examined by bright-field microscopy (×20 and ×40 objectives) to determine the presence of endogenous and exogenous *C. parvum* stages (11).

Microscopy. Microscopy was performed with an Olympus BH2 microscope equipped with epifluorescence and DIC optics, using the following filter sets: 350-nm excitation and 450-nm emission (sky blue) for DAPI, 480-nm excitation and 520-nm emission (bottle green) for FITC-conjugated antibodies, and 500-nm excitation and 630-nm emission (red) for TR-CmAb. Photography was performed using a ColorView (Soft Imaging Systems Inc.) digital camera attached to an Olympus BH2 microscope, and all images shown represent results of at least three experiments. All oocyst enumerations were performed at a total magnification of either ×500 or ×1,250, and the localization of all fluorogens and organelles was investigated at a total magnification of ×1,250.

Statistical analysis. Statistical analysis was performed by analysis of variance (ANOVA) with $P < 0.05$ as the criterion of significance by using the MINITAB version 11 program. The analysis of oocyst infectivity in the neonatal mouse employed the calculation of the logit dose response and dose response curves as described by Korich et al. (11).

RESULTS

Labeling nuclei of irradiated, excysted sporozoites with anti-thymine dimers antibodies. Irradiated sporozoites, purified from oocysts exposed to a 40-mJ · cm^{-2} dose of UV light, were treated with anti-TDmAb and FITC-labeled anti-mouse IgG. Sporozoite nuclei were also stained with DAPI, and their images are shown in Fig. 1. Evidence for TD localization in the nuclei of irradiated sporozoites was obtained: both anti-TDmAb and DAPI colocalized in the nuclei of irradiated sporozoites (Fig. 1A), but only DAPI localized in the nuclei of nonirradiated (control) sporozoites (Fig. 1B). Irradiated sporozoites treated with anti-dsDNAmAb acted as positive controls. Anti-dsDNAmAb binding localized in the nuclei of both irradiated and nonirradiated sporozoites (Fig. 1C and D), whereas anti-TDmAb labeling was restricted to the nuclei of irradiated sporozoites (Fig. 1A and B). Sporozoite external surfaces, but not nuclei, of both irradiated and control sporozoites bound anti-CspAb homogeneously (Fig. 1E and F). Similar results were obtained when irradiated and control sporozoites were treated with an "in-house" rabbit anti-*Cryptosporidium* sp. oocyst extract polyclonal antibody (data not shown).

We estimated the percent binding of anti-TDmAb to the nuclei of irradiated sporozoites after different membrane permeation treatments. The percent binding ranged between ~10 and ~60% with PFA, microwaving, or heating in a water bath at 70°C (Table 1). Maximal antibody binding to sporozoite nuclei (>80%) was achieved when irradiated sporozoites were air dried on slides overnight at RT prior to methanol fixation (Table 1).

Freezing and thawing of irradiated oocysts. Freezing and thawing of irradiated *C. parvum* and *C. hominis* oocysts facilitated the inclusion of anti-TDmAb into sporozoite nuclei localized within oocysts. *C. parvum* or *C. hominis* oocysts irradiated with 40 mJ · cm^{-2} were used to determine the effect of the number of freeze-thaw cycles on the efficiency of anti-TDmAb binding in individual oocysts by using oocysts which were either freeze-thawed in suspension and then air dried on microscope slides or air dried on microscope slides and then freeze-thawed. Initially, 7 cycles of freezing and thawing (representing ~50%) of the 15 recommended cycles used by Nichols and Smith (14) were used with both oocyst suspensions and air-dried oocysts. Irradiated samples showed specific nuclear localization of anti-TDmAb, which was absent in the control group (Fig. 2A and B). Irradiated *C. parvum* and *C. hominis* oocysts exhibited the same labeling pattern with anti-TDmAb (data not shown).

Oocysts exposed to 10 freeze-thaw cycles showed large numbers of disrupted, empty oocysts with their sporozoites scattered at a distance outside the empty oocysts, whereas oocysts exposed to 5 or 7 cycles exhibited disrupted oocysts, with the majority of sporozoites still localized within. We estimated the percentage of binding of anti-TDmAb to the nuclei of irradiated sporozoites localized within disrupted oocysts after 5, 7, or 10 freeze-thaw cycles. The percentage of binding ranged between ~99 and 100% for all freeze-thaw cycles tested. Only intact oocysts with undisrupted oocyst walls showed no binding to anti-TDmAb. As there were no significant differences between 5, 7, or 10 cycles with respect to the numbers of oocysts disrupted and the percentages of binding of anti-TDmAb to the nuclei of sporozoites within the irradiated oocysts (Table 2), we used 5 freeze-thaw cycles, to retain the majority of sporozoites within their respective oocysts, in all further experiments.

Maximizing the user friendliness of the assay. Freezing and thawing of irradiated *C. parvum* and *C. hominis* oocysts either in suspension or after air drying on microscope slides produced similar and efficient labeling patterns with anti-TDmAb and DAPI. We maximized the user friendliness of the assay by air drying irradiated oocysts on slides for all further experiments, as this procedure is also undertaken for the identification and enumeration of *Cryptosporidium* sp. oocysts in both United Kingdom and U.S. standard methods (2, 3, 24, 25). Also, in addition to anti-TDmAb and DAPI labeling, we labeled oocyst walls with a commercially available FITC-CmAb so that oocysts could be recognized readily. Irradiated oocysts bound both anti-TDmAb and FITC-CmAb, whereas control oocysts bound FITC-CmAb only (Fig. 2C and D).

Influence of age and viability on the generation and/or detection of thymine dimers following UV light damage. Recently excreted and aged *C. parvum* oocysts were irradiated with 40 mJ · cm^{-2} as described above. Controls consisting of nonirradiated samples were also prepared from each group. Prior to UV irradiation, oocyst viability was assessed using a fluorogenic vital dye assay (6). The percent viability of recently ex-

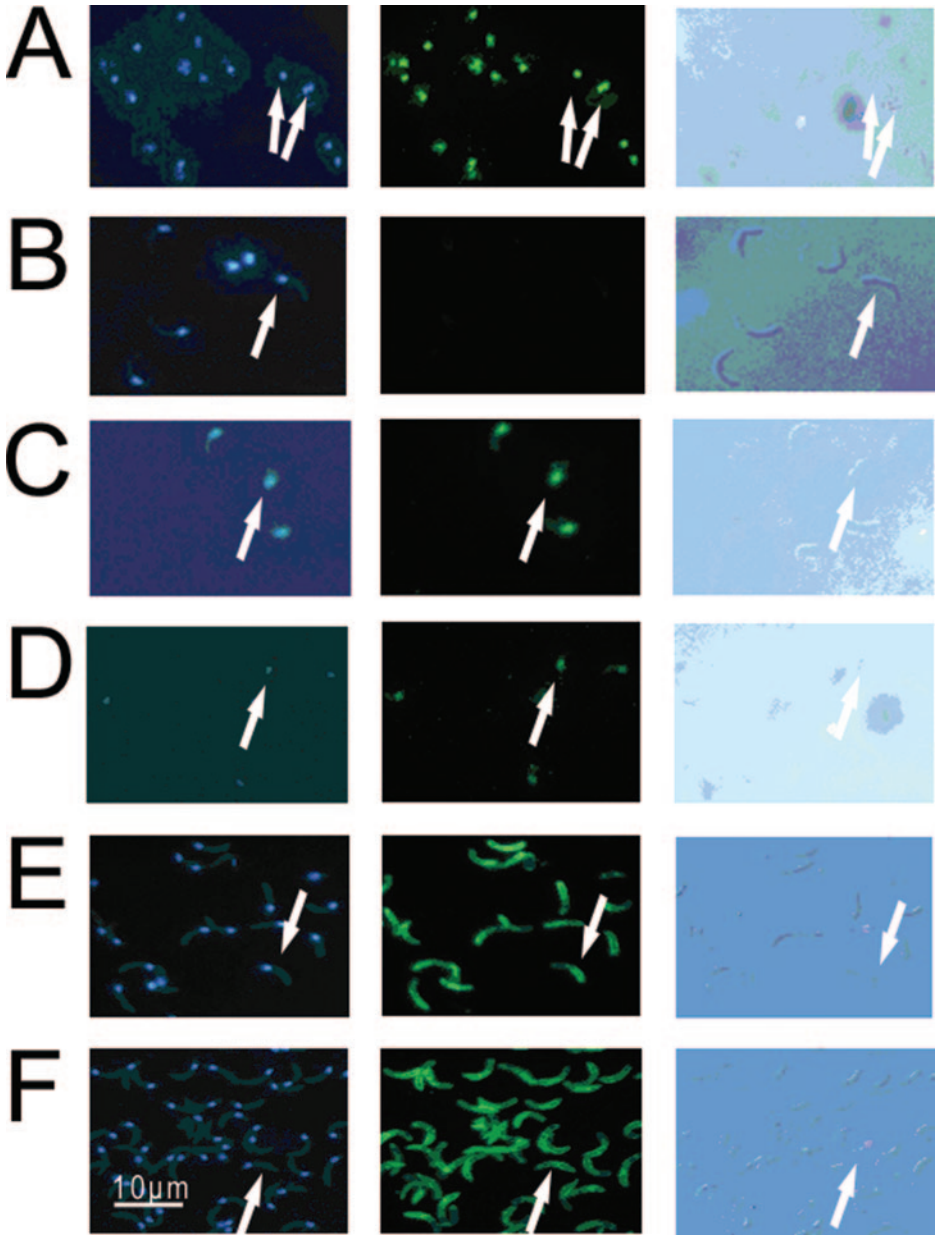

FIG. 1. The effect of irradiation on the labeling of sporozoite nuclei with three different antibodies. Irradiated sporozoites were purified from *C. parvum* oocysts exposed to a 40-mJ · cm^{-2} dose of UV light. Sporozoites were air dried on microscope slides, fixed in methanol, and labeled with specific antibodies (see below) and DAPI. Sporozoites were visualized by Nomarski differential interference contrast optics (images in left column) and by fluorescence microscopy using a blue filter set (emission, 461 nm) for DAPI (middle column) and a green filter set (emission, 518 nm) for FITC-labeled antibodies (right column). (A and B) Irradiated sporozoites (A) and controls (B) labeled with anti-TDmAb. (C and D) Irradiated sporozoites (C) and controls (D) labeled with anti-dsDNAmAb. (E and F) Irradiated sporozoites (E) and controls (F) labeled with anti-CspAb. Arrows point to the nuclear localization of the fluorescent products at the posterior end of sporozoites.

creted oocysts was 92%, compared to 5% for the aged group. The viable and dead oocysts in the irradiated samples bound anti-TDmAb (Fig. 2A) identically, while control (recently excreted and aged) oocysts failed to bind anti-TDmAb (Fig. 2B).

Effect of different UV irradiation doses of intact oocysts on anti-TDmAb binding. Oocysts exposed to 40 mJ · cm^{-2} and labeled with anti-TDmAb, FITC-CmAb, and DAPI demonstrated clear nuclear labeling with anti-TDmAb. Oocysts exposed to 4, 10, or 20 mJ · cm^{-2} and labeled with anti-TDmAb, FITC-CmAb, and DAPI failed to demonstrate clear nuclear labeling with anti-TDmAb. However, these oocysts demonstrated clear anti-TDmAb nuclear labeling when the FITC-CmAb labeling step was omitted. Thus, in oocysts exposed to low (4- to 20-mJ · cm^{-2}) levels of UV irradiation, the addition of the FITC-CmAb step interfered with the detection of FITC emissions from the anti-TDmAb/FITC-labeled rabbit anti-mouse IgG complex used to visualize TD localization. In all further experiments, FITC-CmAb was replaced with TR-

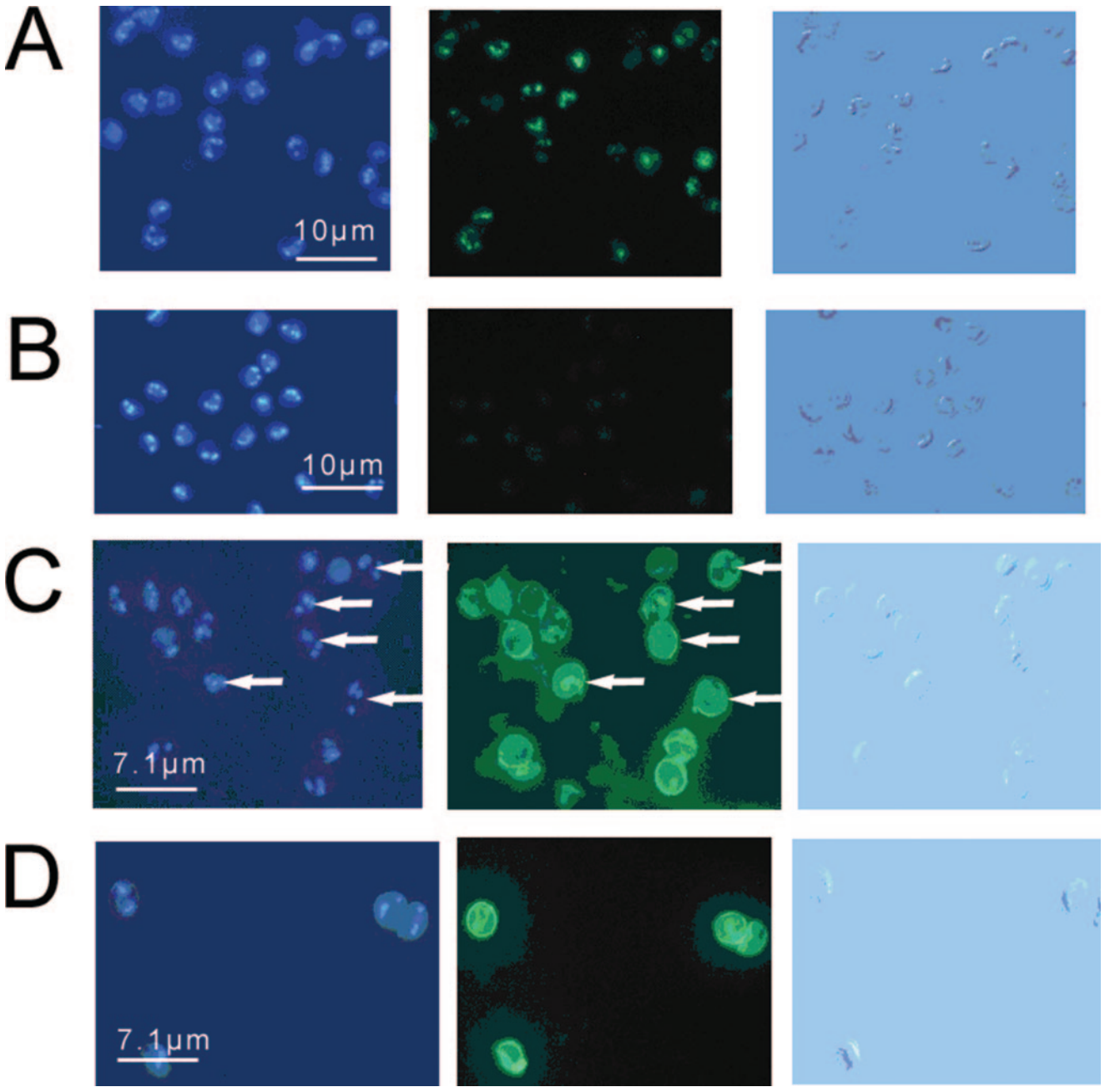

FIG. 2. Labeling of freeze-thawed *C. parvum* oocysts with anti-TDmAb. Oocysts were irradiated at a dose of 40 mJ · cm^{-2} of UV light, frozen, and thawed and labeled with anti-TDmAb and DAPI (A and B) or with a combination of anti-TDmAb, FITC-CmAb, and DAPI (C and D). Panels A and C show irradiated oocysts, whereas panels B and D show nonirradiated controls. Arrows point to the nuclear localization of the fluorescent products at the posterior end of sporozoites within oocysts. Oocysts were stained with DAPI (images in left column) and FITC-labeled-anti-TD antibody (middle column). The right column shows the same images viewed under Nomarski differential interference contrast optics.

CmAb for labeling oocysts exposed to low-level UV irradiation. The combination of TR-CmAb, anti-TDmAb, and DAPI enabled us to visualize specific binding to TD in the nuclei of irradiated oocysts. Binding could be demonstrated after irradiation at 40 mJ · cm^{-2} (Fig. 3A), 20 mJ · cm^{-2} (Fig. 3B), and 10 mJ · cm^{-2} (Fig. 3C) but not at 4 mJ · cm^{-2} (Fig. 3D). Control oocysts did not bind anti-TDmAb (Fig. 3E).

Effect of UV irradiation on the viability of *C. parvum* oocysts. The fluorogenic vital dye assay (6) and the maximized in vitro excystation method (17) were used to evaluate the effectiveness of UV irradiation at doses of 10, 20, or 40 mJ · cm^{-2} on the viability of *C. parvum* oocysts. Both methods failed to demonstrate significant changes in the viability of irradiated compared to nonirradiated oocysts (the percent viable in the irradiated group [mean ± standard deviation {SD}] was 93.0 ± 3.0 at 10 mJ · cm^{-2}, 89.7 ± 0.6 at 20 mJ · cm^{-2}, or 86.0 ± 6.1 at 40 mJ · cm^{-2}, and the percent viable in the control group [mean ± SD] was 87.0 ± 4.4, 89.7 ± 5.9, or 89.7 ± 2.5,

TABLE 2. Percent disrupted oocysts and percent binding of anti-TDmAb to the nuclei of irradiated sporozoites in *C. parvum* and *C. hominis* oocysts[a]

No. of freeze-thaw cycles	% Disrupted oocyst[b,c]		% Antibody binding[b,d]	
	C. parvum	*C. hominis*	*C. parvum*	*C. hominis*
5	97.3 ± 0.2	96.5 ± 1.0	99.3 ± 0.7	99.6 ± 0.4
7	97.2 ± 1.0	95.3 ± 0.7	100 ± 0.0	99.0 ± 1.0
10	98.1 ± 1.3	97.6 ± 2.1	99.0 ± 1.0	99.6 ± 0.4

[a] *C. parvum* and *C. hominis* oocysts were air dried on microscope slides and exposed to different numbers of cycles of freezing and thawing. The disruption of oocysts and their contents was visualized by labeling with FITC-CmAb and DAPI. The binding of anti-TDmAb to the nuclei of irradiated sporozoites within oocysts was visualized by labeling with anti-TDmAb, DAPI, and FITC-CmAb. Samples were examined by epifluorescence and Nomarski DIC microscopy.

[b] Results are given as means ± SDs. The mean percentage was obtained by enumerating 300 oocysts per treatment ($n = 3$). Results are not statistically significantly different at $P < 0.05$.

[c] Disrupted oocysts had a morphological break in the perimeter of the oocyst wall (Fig. 2, images in columns 2 and 3; Fig. 3, images in columns 3 and 4).

[d] Percent antibody binding indicates the number of oocysts containing sporozoites with anti-TDmAb$^+$, DAPI$^+$ nuclei ($n = 300$ observations per sporozoite treatment).

respectively; $P > 0.05$). For the maximized in vitro excystation assay, oocyst viability was as follows: for the irradiated group, the mean ± SD was 95.7 ± 0.6 at 10 mJ · cm^{-2}, 91.0 ± 2.6 at 20 mJ · cm^{-2}, or 93.0 ± 1.5 at 40 mJ · cm^{-2}; for the control group, the mean ± SD was 96.0 ± 1.7, 94.3 ± 1.5, or 93.3 ± 2.1, respectively; $P > 0.05$.

Effect of different UV irradiation doses of intact oocysts on neonatal mouse infectivity. (i) Determination of infectious doses. The number of oocysts present in 10-μl doses administered by gavage to neonatal mice was confirmed by immunofluorescence microscopy. The number of oocysts enumerated in infectious doses of 300 or 3,000 UV-treated oocysts ranged between 225 and 234 and 2,511 and 2,480, respectively. For the nonirradiated oocysts used to construct the standard curve, the number present in 10-μl doses ranged between 12 and 21, 58 and 110, and 180 and 265 for infectious doses of 30, 150, and 300, respectively.

(ii) Determination of infection. In infected neonates, endogenous stages were localized readily within the brush border of the intestinal villi, and oocysts were present in the lumen. Slides were scored as positive or negative according to the presence or absence of *C. parvum* life cycle stages. Neonates infected with 300 or 3,000 oocysts irradiated at either 10 or 20 mJ · cm^{-2} showed no histopathological evidence of *C. parvum* infection, whereas those infected with nonirradiated oocysts showed various levels of infection. In these standard curve groups, the percentage of infection ranged from 5.2% in neonates infected with 30 oocysts to 80% in neonates infected with 300 oocysts (Fig. 4).

Comparison of the neonatal mouse infectivity assay with the anti-TDmAb immunofluorescence assay. Neonates infected with 300 or 3,000 oocysts irradiated at either 10 or 20 mJ · cm^{-2} showed no evidence of infection, whereas various numbers of neonates infected with doses of 30, 150, or 300 oocysts became infected (Fig. 4). Sporozoite nuclei within oocysts irradiated at either 10 or 20 mJ · cm^{-2} bound anti-TDmAb, whereas sporozoite nuclei within oocysts that were not irradiated (control) did not bind anti-TDmAb (Fig. 3).

DISCUSSION

UV light damages DNA, and the major lesions induced are CPD. TDs are common forms of CPD produced in cells when UV light is absorbed by the double bond in the thymine base in a DNA molecule, opening the bond and allowing it to react with the adjacent thymine base, forming a tight four-member ring (12). UV irradiation of *C. parvum* oocysts also produces CPD, and UV inactivation of *C. parvum* and *C. hominis* is irreversible, despite the presence of UV repair genes (10, 16, 18, 19). An assay that can detect the presence of TD following UV inactivation in individual waterborne oocysts would prove beneficial to the water industry, public health professionals, and government regulators. We developed a fluorescence-based localization system for detecting TD in irradiated *C. parvum* and *C. hominis* oocysts using a commercially available anti-TDmAb. Dimer-specific fluorescence localization in sporozoite nuclei was confirmed by colocalization with the nuclear fluorogen DAPI.

In our assay, fixed microscopic preparations of UV-irradiated oocysts and purified sporozoites were labeled with anti-TDmAb, the binding of which was detected by using fluorescent, species-specific secondary antibodies. Oocyst walls were visualized by using commercially available, genus-specific, fluorescence-labeled monoclonal antibodies reactive with exposed epitopes in/on oocyst walls. To our knowledge, this is the first description of an immunofluorescence-based assay to detect UV damage by localizing TD in the nuclei of both irradiated, purified sporozoites and sporozoites within oocysts of *C. parvum* and *C. hominis*.

Experimental evidence for the presence of TD in irradiated *C. parvum* oocysts is limited. Oguma et al. (16) conducted an endonuclease-sensitive site assay to determine the presence of UV-induced pyrimidine dimers in *C. parvum* genomic DNA. Using a chemiluminescence-based Western blot assay, Rochelle et al. (19) demonstrated the accumulation of TD in the *C. parvum* genome when oocysts were exposed to various doses of UV light (3 to 104 mJ · cm^{-2}). Our data demonstrate the validity and usefulness of fluorescence and immunofluorescence to detect TD in the nuclei of irradiated sporozoites contained within *C. parvum* and *C. hominis* oocysts. Molecular and immunoblotting methods are regarded as more sensitive than immunofluorescence-based methods. However, our method has its advantages. First, the morphology of oocysts is preserved, permitting the examination of individual oocysts or sporozoites by DIC. Second, the immunofluorescence labeling method can be used with samples air dried on slides, consistent with both United Kingdom Drinking Water Inspectorate (2, 3) and U.S. EPA (24, 25) requirements for analyzing water for the presence of *Cryptosporidium* sp. oocysts. Third, the use of both positive (anti-dsDNA) and negative (nonirradiated oocysts) controls increases the accuracy of the assay.

When we used FITC as a reporter for both the unlabeled primary antibody (mouse anti-TDmAb and FITC-labeled rabbit anti-mouse IgG) and the oocyst wall (FITC-CmAb), visualization of anti-TDmAb localization in sporozoite nuclei at UV doses below 40 mJ · cm^{-2} became difficult, as the emission from FITC-CmAb obscured that of the indirectly labeled anti-TDmAb, being more intense and appearing as increased background staining. Thus, when oocysts were exposed to low (4- to

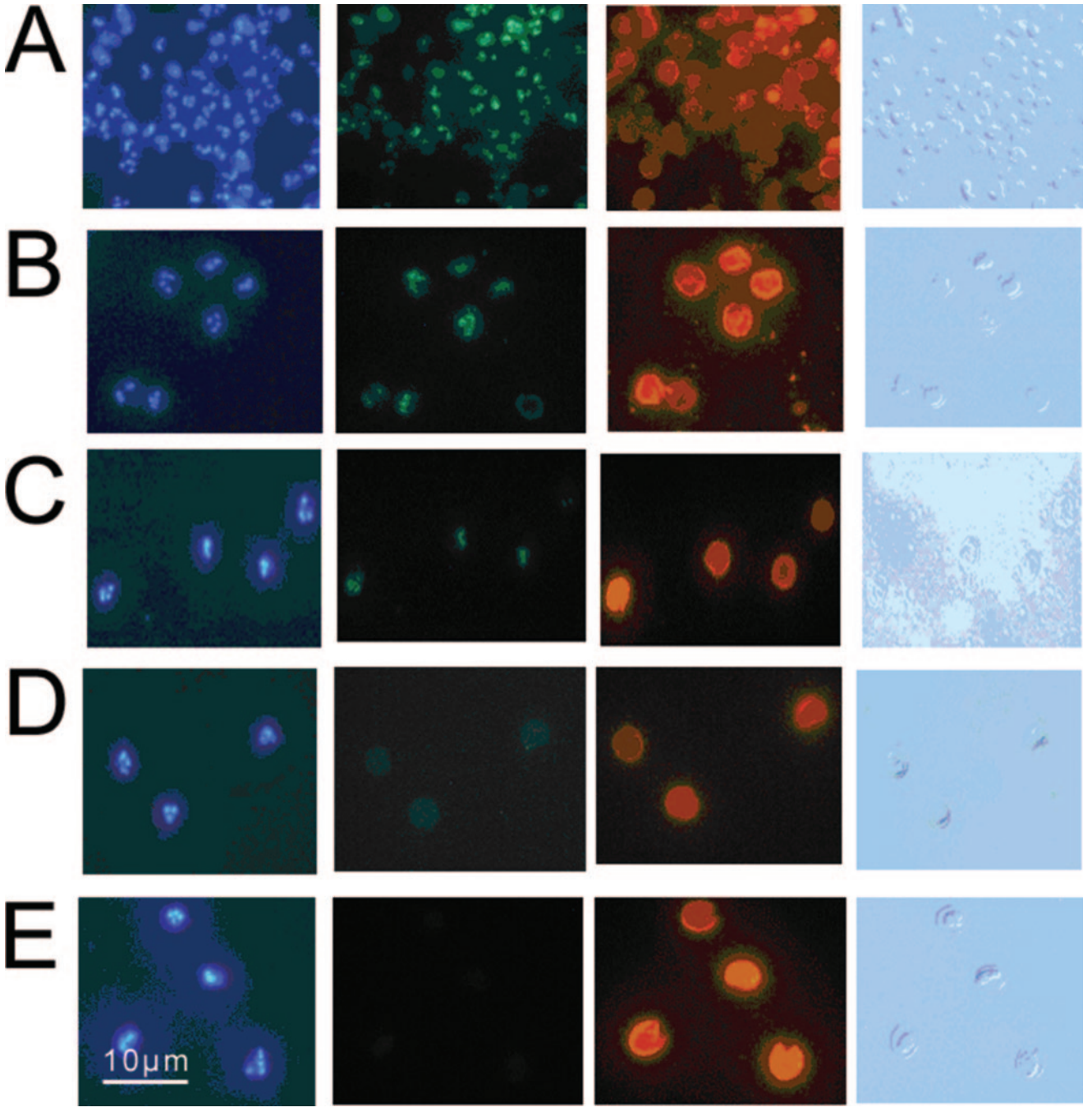

FIG. 3. The effect of different doses of irradiation on anti-TDmAb labeling of *C. parvum* oocysts. (A to D) Oocysts exposed to 40 mJ · cm^{-2} (A), 20 mJ · cm^{-2} (B), 10 mJ · cm^{-2} (C), and 4 mJ · cm^{-2} (D) of UV light. (E) Control, nonirradiated oocysts. Oocysts in both irradiated and control groups were labeled with a combination of anti-TDmAb, TR-CmAb, and DAPI, and the images are presented in four columns. First column, DAPI localization; second column, FITC-anti-TDmAb localization; third column, TR-CmAb; fourth column, Nomarski differential interference contrast microscopy image.

20-mJ · cm^{-2}) levels of UV irradiation and stained with FITC-CmAb, we could not detect FITC emissions from the indirectly labeled anti-TDmAb, although anti-TDmAb localization was readily detectable at 10 and 20 mJ · cm^{-2} in the absence of the FITC-CmAb step. As FITC-CmAb interfered with the detection of FITC emissions from the indirectly labeled anti-TDmAb, this technical issue was overcome by replacing FITC-CmAb with TR-CmAb in further studies.

Previous studies have shown that *C. parvum* oocysts can be inactivated by low (<10-mJ · cm^{-2}) doses of UV light using low- or medium-pressure UV lamps (7, 16, 18, 22). We observed nuclear, anti-TD binding in oocysts irradiated at 40, 20,

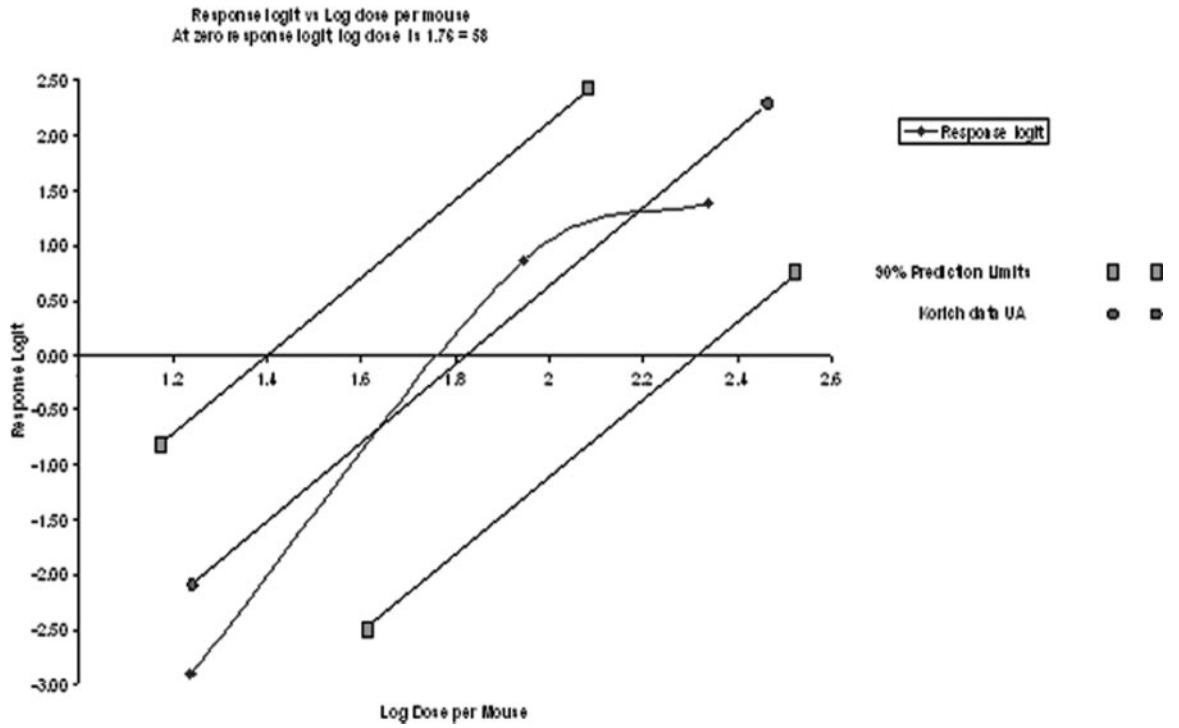

FIG. 4. Dose-response curves for nonirradiated oocysts of the Iowa isolate of *C. parvum* in CD-1 mice. Infectivity was measured for the 10- or 20-mJ · cm^{-2}-irradiated oocysts and control, nonirradiated oocysts (◆). Oocysts irradiated with 10 or 20 mJ · cm^{-2} of UV light in this study were not infectious to neonatal CD-1 mice. ●, response logit versus log dose per mouse for data from Korich et al. of the University of Alabama (UA) (11). ■, 90% confidence limits of response logit versus log dose per mouse for data from reference 11.

and 10 mJ · cm^{-2} but not in oocysts irradiated at <10 mJ · cm^{-2}. Our assay should work when medium to high doses of UV irradiance (range, 10 to 40 mJ · cm^{-2}) are used, but its sensitivity is limited, currently, if doses as low as 4 mJ · cm^{-2} are used to dose *Cryptosporidium*-contaminated potable water. Assay sensitivity can be increased, for example, by (i) direct labeling of whole anti-TDmAb molecules, (ii) generating Fab or $(Fab)_2$ anti-TDmAb fragments to increase paratope/epitope interaction, (iii) increasing the fluorescein-to-protein ratio of the antibodies, and (iv) using confocal microscopy to visualize and localize fluorescent images.

Our current understanding of the effectiveness of UV irradiation in the inactivation of *C. parvum* oocysts is based on both animal infectivity and cell culture assays (4, 16, 22). The experiments reported here, using the fluorogenic vital dye assay and the maximized in vitro excystation assay, do not provide supportive evidence for the inactivation of *C. parvum* oocysts following exposure to 10, 20, and 40 mJ · cm^{-2} doses of UV irradiation. There is agreement in the literature that in vitro viability assays can overestimate oocyst viability compared with animal infectivity (19). We compared results of anti-TDmAb immunofluorescence localization and the neonatal mouse infectivity assay, using *C. parvum* oocysts irradiated with either 10 or 20 mJ · cm^{-2}. Our data indicate that irradiated oocysts failed to cause infection in neonatal CD-1 mice despite the fact that we used higher doses (up to 3,000 per os, which is greater than 30 times the 50% infective dose for this strain of mouse (11). Thus, based on our current neonatal mouse infectivity data and previously published neonatal mouse infectivity data on UV irradiation of *C. parvum* oocysts (4, 7, 8, 13, 18, 19, 22), results of our anti-TDmAb immunofluorescence localization method correlate with those of the neonatal mouse infectivity assay, following exposure to low doses of UV irradiation.

Our data indicate that UV irradiation of viable, infectious, as well as dead oocysts induces DNA damage demonstrated by anti-TDmAb immunofluorescence localization. Regardless of the viability of waterborne oocysts, this assay can demonstrate the effect of exposure of viable and dead oocysts to 10 to 40 mJ · cm^{-2} of UV irradiation by determining the presence of TD in *C. parvum* and *C. hominis* oocysts. Thus, the effect of UV irradiation in water treatment processes can be determined for all *C. parvum* and *C. hominis* oocysts.

Given that *C. parvum* and *C. hominis* are the major species causing human cryptosporidiosis, few studies have been conducted into the effects of UV irradiation on *C. hominis* oocysts, as this species is difficult to propagate in animal models (26). Using a combination of data mining and DNA sequencing, Rochelle et al. (18) demonstrated that *C. hominis* oocysts express genes to repair UV-induced pyrimidine dimers in their genomic DNA. Johnson et al. (10) used cell culture-based methods to measure the infectivity and inactivation of UV-irradiated *C. hominis* oocysts and concluded that *C. hominis* oocysts displayed similar levels of infectivity and had the same sensitivity to UV light as *C. parvum*. Our findings indicate not only that *C. hominis* and *C. parvum* oocysts display similar levels of UV light sensitivity but also that irradiated *C. hominis*

oocysts exhibit the same anti-TDmAb immunofluorescence localization pattern as *C. parvum.*

ACKNOWLEDGMENTS

This work was funded by the Environmental and Rural Affairs Department, Agricultural and Biological Research Group, Scottish Executive, Scotland, United Kingdom.

We thank D. Reid, Drinking Water Quality Unit, Scottish Executive, 1-H(N) Victoria Quay, Edinburgh EH6 6QQ, United Kingdom, for managing the project.

REFERENCES

1. **Anonymous.** 1999. Isolation and identification of *Cryptosporidium* oocysts and *Giardia* cysts in waters, 1999. Methods for the examination of waters and associated materials. HMSO, London, United Kingdom.
2. **Anonymous.** 1999. The water supply (water quality) (amendment). Regulations 1999, SI no. 1524. Drinking Water Inspectorate, London, United Kingdom.
3. **Anonymous.** 2005. Standard operating protocol for the monitoring of *Cryptosporidium* oocysts in treated water supplies to satisfy The Water Supply (Water Quality) Regulations 200, SI no. 3184 England/The Water Supply (Water Quality) Regulations 2001, SI no. 3911 (W.323) Wales. Part 2. Laboratory and analytical procedures. Drinking Water Inspectorate, London, United Kingdom. http://www.dwi.gov.uk/regs/crypto/pdf/sop%20part%202.pdf.
4. **Belosevic, M., S. A. Craik, J. L. Stafford, N. F. Neumann, J. Kruithof, and D. W. Smith.** 2001. Studies on the resistance/reactivation of *Giardia muris* cysts and *Cryptosporidium parvum* oocysts exposed to medium-pressure ultraviolet irradiation. FEMS Microbiol. Lett. **204:**197–204.
5. **Bukhari, Z., and H. V. Smith.** 1995. Effect of three concentration techniques on viability of *Cryptosporidium parvum* oocysts recovered from bovine feces. J. Clin. Microbiol. **33:**2592–2595.
6. **Campbell, A. T., L. J. Robertson, and H. V. Smith.** 1992. Viability of *Cryptosporidium parvum* oocysts: correlation of in vitro excystation with inclusion or exclusion of fluorogenic vital dyes. Appl. Environ. Microbiol. **58:**3488–3493.
7. **Craik, S. A., D. Weldon, G. R. Finch, J. R. Bolton, and M. Belosevic.** 2001. Inactivation of *Cryptosporidium parvum* oocysts using medium- and low-pressure ultraviolet radiation. Water Res. **35:**1387–1398.
8. **Hijnen, W. A. M., E. F. Beerendonk, and G. J. Medema.** 2006. Inactivation credit of UV irradiation for viruses, bacteria and protozoan (oo)cysts in water: a review. Water Res. **40:**3–22.
9. **Homan, W., T. Van Gorkom, Y. Y. Kan, and J. Hepener.** 1999. Characterization of *Cryptosporidium parvum* in human and animal feces by single-tube nested polymerase chain reaction and restriction analysis. Parasitol. Res. **85:**707–712.
10. **Johnson, A. M., K. Linden, K. M. Ciociola, R. De Leon, G. Widmer, and P. A. Rochelle.** 2005. UV inactivation of *Cryptosporidium hominis* as measured in cell culture. Appl. Environ. Microbiol. **71:**2800–2802.
11. **Korich, D. G., M. M. Marshall, H. V. Smith, J. E. O'Grady, Z. Bukhari, C. R. Fricker, J. P. Rosen, and J. L. Clancy.** 2000. Inter-laboratory comparison of the CD-1 neonatal mouse logistic dose-response model for *Cryptosporidium parvum* oocysts. J. Eukaryot. Microbiol. **47:**294–298.
12. **Mitchell, D. L.** 1988. The relative cytotoxicity of (6-4) photoproducts and cyclobutane dimers in mammalian cells. Photochem. Photobiol. **48:**51–57.
13. **Morita, S., A. Namikoshi, T. Hirata, K. Oguma, H. Katayama, S. Ohgaki, N. Motoyama, and M. Fujiwara.** 2002. Efficacy of UV irradiation in inactivating *Cryptosporidium parvum* oocysts. Appl. Environ Microbiol. **68:**5387–5393.
14. **Nichols, R. A. B., and H. V. Smith.** 2004. Optimization of DNA extraction and molecular detection of *Cryptosporidium* oocysts in natural mineral water sources. J. Food Prot. **67:**524–532.
15. **Nichols, R. A. B., B. M. Campbell, and H. V. Smith.** 2003. Identification of *Cryptosporidium* spp. oocysts in United Kingdom noncarbonated natural mineral waters and drinking waters by using a modified nested PCR-restriction fragment length polymorphism assay. Appl. Environ. Microbiol. **69:**4183–4189.
16. **Oguma, K., H. katayama, H. Mitani, S. Morita, T. Hirata, and S. Ohgaki.** 2001. Determination of pyrimidine dimers in *Escherichia coli* and *Cryptosporidium parvum* during UV light inactivation, photoreactivation, and dark repair. Appl. Environ. Microbiol. **67:**4630–4637.
17. **Robertson, L. J., A. T. Campbell, and H. V. Smith.** 1993. *In vitro* excystation of *Cryptosporidium parvum*. Parasitology **106:**13–19.
18. **Rochelle, P. A., D. Fallar, M. M. Marshall, B. A. Montelone, S. J. Upton, and K. Woods.** 2004. Irreversible UV inactivation of *Cryptosporidium* spp. despite the presence of repair genes. J. Eukaryot. Microbiol. **51:**553–562.
19. **Rochelle, P. A., S. J. Upton, B. A. Montelon, and K. Woods.** 2005. The response of *Cryptosporidium* to UV light. Trends Parasitol. **21:**81–87.
20. **Rothschild, L. J.** 1999. The influence of UV radiation on protistan evolution. J. Eukaryot. Microbiol. **46:**548–555.
21. **Roza, L., F. R. De Gruijl, J. B. A. Bergen Henegouwen, K. Guikers, H. Van Weelden, G. P. Van Der Schans, and R. A. Baan.** 1991. Detection of photorepair of UV-induced thymine dimers in human epidermis by immunofluorescence microscopy. J. Investig. Dermatol. **96:**903–907.
22. **Shin, G. A., K. G. Linden, M. J. Arrowood, and M. D. Sobsey.** 2001. Low-pressure UV inactivation and DNA repair potential of *Cryptosporidium parvum* oocysts. Appl. Environ. Microbiol. **67:**3029–3032.
23. **Smith, H. V., B. M. Campbell, C. A. Paton, and R. A. B. Nichols.** 2002. Significance of enhanced morphological detection of *Cryptosporidium* sp. oocysts in environmental water concentrates using DAPI and immunofluorescence microscopy. Appl. Environ. Microbiol. **68:**5198–5201.
24. **U.S. Environmental Protection Agency.** 2001. Method 1622: *Cryptosporidium* in water by filtration/IMS/FA, EPA 821-R01-026. Office of Water, U.S. Environmental Protection Agency, Washington, DC.
25. **U.S. Environmental Protection Agency.** 2001. Method 1623: *Giardia* and *Cryptosporidium* in water by filtration/IMS/FA, EPA 821-R01-025. Office of Water, U.S. Environmental Protection Agency, Washington, DC.
26. **Widmer, G., D. Akiyoshi, M. A. Buckholt, X. Feng, S. M. Rich, K. M. Deary, C. A. Bowman, P. Xu, Y. Wang, G. A. Buck, and S. Tzipori.** 2000. Animal propagation and genomic survey of a genotype 1 isolate of *Cryptosporidium parvum*. Mol. Biochem. Parasitol. **108:**187–197.
27. **Xiao, L., L. Escalante, C. Young, I. Sulaiman, A. A. Escalante, J. R. Montali, R. Fayer, and A. A. Lal.** 1999. Phylogenetic analysis of *Cryptosporidium* parasites based on the small-subunit rRNA gene locus. Appl. Environ. Microbiol. **65:**1578–1583.
28. **Xiao, L., K. Alderisio, J. Limor, M. Royer, and A. A. Lal.** 2000. Identification of species and sources of *Cryptosporidium* oocysts in storm waters with a small-subunit rRNA-based diagnostic and genotyping tool. Appl. Environ. Microbiol. **66:**5492–5498.